

# INTERPLAY OF CELL-CELL SIGNALLING AND MULTICELLULAR MORPHOGENESIS DURING DICTYOSTELIUM AGGREGATION

THOMAS HÖFER, PHILIP K. MAINI

Centre for Mathematical Biology,  
Mathematical Institute, University of Oxford  
24-29 St Giles', Oxford OX1 3LB, UK

## 1 Introduction

The cellular slime mould *Dictyostelium discoideum* provides a paradigm model system for the study of multicellular pattern formation. Its life cycle involves a route to primitive multicellular organization which has independently evolved in terrestrial species of at least four groups of microorganisms (myxobacteria, acrasiomycota—the cellular slime moulds, myxomycota, and ciliata [1]). In these species a large number of single cells (nuclei in myxomycota) form, through a process of aggregation and differentiation, a fruiting body.

Of these *Dictyostelium* in particular has been the subject of much experimental and theoretical research; a detailed description of its life cycle can be found for example in [2]. Briefly, under favourable conditions *Dictyostelium* exists in the form of single amoeboid cells which feed on bacteria in the soil and multiply. Eventually this leads to the exhaustion of the bacterial food sources, which induces cells to actively aggregate into streams. The cell streams coalesce into mounds containing typically  $10^4$ – $10^5$  cells. Passing through a migratory slug-like stage during which cells differentiate in prespore and prestalk cells (and a number of other cell (sub)types), a fruiting body develops. It aids the dispersal of the spores which then develop again into single amoebae.

Here we focus specifically on the aggregation stage; cf. for example Figure 1 in [10]. Cell-cell communication via macroscopic waves of cyclic adenosine 3',5'-monophosphate (cAMP) organizes periodic cell movement towards the aggregation centres [3,4]. These chemical waves take the form of rotating spirals ([10], Figure 1 (a)). The cell layer becomes divided into aggregation territories ([10], Figure 1 (b)), and eventually amoebae form a conspicuous pattern of branching cell streams which radiate from the aggregation centre outwards ([10], Figure 1 (c)). Cell streaming is accompanied by the establishment of direct cell-cell contacts and thus marks the onset of multicellular organization in *Dictyostelium*.

The purpose of the present paper is to integrate the available experimental

information at the cellular level into a quantitative model of the aggregation phase in this ensemble of communicating cells. By means of this model we attempt to show how the individual cell properties conspire to produce the sequence of patterning events observed during aggregation. Particular emphasis will be given to the interaction of intercellular signalling and motile cell behaviour which will turn out to be at the heart of the cell streaming phenomenon.

## 2 Individual cell behaviour

Experimental research on *Dictyostelium* has elucidated many of the cellular and molecular mechanisms involved in morphogenesis and differentiation. Subsequent to starvation cells acquire aggregation competence through the expression of a number of gene products. These equip cells with the ability (1) to synthesize cAMP in an "autocatalytic" feedback loop which plays a central role in establishing long-range cell communication, and (2) to react mechanically to cAMP with directed movement towards increasing cAMP concentration (positive chemotaxis). In particular, elements of the cAMP signalling system are expressed which are responsible for sensing (cAMP receptors), synthesizing (adenylate cyclase, AC) and degrading (cAMP-phosphodiesterases, PDE) cAMP [5]. The major cAMP receptor type, cAR1, also mediates the chemotactic response. In addition, other components of the AC and chemotactic pathways, such as specific G-proteins, accumulate after starvation [6].

A central feature of both pathways is their activation as well as desensitization by cAMP. This is particularly well characterized in the case of the AC pathway. Binding of extracellular cAMP to the cAMP receptors leads to a relatively fast G-protein mediated activation of AC, and the synthesized cAMP is rapidly transported into the extracellular medium (response time of the order of seconds). This provides a self-enhancement mechanism for the cAMP signal. The "autocatalytic" response is terminated by a desensitization (adaptation) of the pathway to further stimulation, brought about by cAMP on a somewhat slower timescale (order of minutes). Multiple desensitization mechanisms have been characterized [7]; most relevant for the timecourse of the cAMP signals during aggregation appears to be desensitization at the receptor/G-protein level.

Activation of the chemotactic pathway follows a very similar pattern [8]. Here inositol 1,4,5-trisphosphate, calcium and cyclic GMP function as intracellular messengers linking the cAMP receptors to the motile machinery of the cell. Again several desensitization mechanisms are known, and it appears that a somewhat faster desensitization reaction than that of the AC pathway is

required to achieve accurate cell orientation [8,9].

## 3 A model of pattern formation in the cellular ensemble

On the basis of this information on individual cell behaviour we can derive a minimal model for pattern formation in the cellular ensemble. The model takes into account three dynamic variables; cell density,  $n(x, y, t)$ , concentration of extracellular cAMP,  $u(x, y, t)$ , and fraction of active cAMP receptors per cell (that is, cellular sensitivity towards the cAMP signal),  $v(x, y, t)$ , all dependent on space,  $(x, y)$ , and time,  $t$ . The evolution equations for these variables take the form [10]

$$\frac{\partial n}{\partial t} = \underbrace{\nabla \cdot (\mu(n)\nabla n)}_{\text{random migration}} - \underbrace{\nabla \cdot (\chi(v)n\nabla u)}_{\text{chemotaxis}}, \quad (1)$$

$$\frac{\partial u}{\partial t} = \lambda \underbrace{[\phi(n)g_+(u, v)]}_{\text{synthesis}} - \underbrace{(\phi(n) + \delta)g_-(u)}_{\text{degradation}} + \underbrace{D\nabla^2 u}_{\text{diffusion}}, \quad (2)$$

$$\frac{\partial v}{\partial t} = \underbrace{-f_+(u)v}_{\text{desensitization}} + \underbrace{f_-(u)(1-v)}_{\text{resensitization}}, \quad (3)$$

where  $\nabla = (\partial/\partial x, \partial/\partial y)$ . We briefly discuss each of these equations in turn.

The dynamics of the cell distribution will be a central element of the model. To monitor it, we introduce the cell density variable  $n$  which can be crudely viewed as a continuous space-dependent average of the (discrete) cell distribution obtained over a characteristic length of a few cell diameters. It is governed by the advection-diffusion equation (1) which accounts for random cell migration ("diffusion"), directed movement in cAMP gradients,  $\nabla u$  (chemotaxis), and, in conjunction with equation (3), for a time-dependent adaptation response towards the cAMP signal. This last feature is realized by the dependence of the chemotactic coefficient  $\chi$  on the fraction of active cAMP receptors,  $v$ . The chemotactic coefficient represents a combined measure of sensitivity to the signal and motile response and should therefore record the effect of adaptation. We choose it to be of the form  $\chi(v) = \chi_0 v^m / (A^m + v^m)$ ,  $m > 1$ , that is, there is a threshold value of active receptors,  $A$ , which is required for efficient sensing of the signal. In [11] we have shown that such an extension of the standard chemotaxis model [12] is necessary if the characteristic timescales of changes in the chemoattractant (cAMP) concentration and adaptation towards the chemoattractant are of comparable magnitudes. This is the case in *Dictyostelium* aggregation (cf. discussion in [11]), and probably ensures that

cells aggregate by rendering cells unresponsive to the cAMP gradient in the wavebacks of the periodic cAMP waves.

Equations (2)–(3) for the signalling dynamics are adapted from a model of cAMP signalling by Martiel & Goldbeter [13–15]. For computational reasons we take somewhat simpler functional forms for the reaction rates  $f_{\pm}$  and  $g_{\pm}$  in equations (2) and (3) than those derived in [13] which, nevertheless, retain the important characteristics of the latter:  $f_{+} = k_{+}u$ ,  $f_{-} = k_{-}$ ,  $g_{+} = (bv + v^2)(a + u^2)/(1 + u^2)$ ,  $g_{-} = du$ . The adaptation and cAMP degradation kinetics follow simple linear or bilinear rate laws, while the rate of the AC pathway ( $g_{+}$ ) accounts for stimulation by cAMP depended on the cellular sensitivity. Estimates for the majority of model parameters can be extracted from the experimental literature [10]; see legends to Figures 1 and 3. In contrast to the original model, which was developed for suspensions of constant cell density, we have to account explicitly for the feedback of the cell distribution into the local cAMP dynamics. As both cAMP synthesis and hydrolysis are linked to cells (intracellular AC pathway, PDE carried on cell membranes), the cAMP production and degradation rates at a certain point in the medium depend on the cell density at this point. This gives rise to the cell density factor  $\phi(n)$  in (2). In general it will be an increasing function of the cell density. Specifically, we take the form  $\phi(n) = n/((1 - \rho n)/(K + n))$ ; see [10] for details. A small background activity of secreted PDE independent of cell density is added ( $\delta$ ).

Equations (2)–(3) with the cell density “clamped” at a constant value essentially reduce to the system investigated by Tyson *et al.* [14] as a model of cAMP signalling at the onset of aggregation. Alternative models for this situation have been developed [16,17]. The models differ in particular with respect to the actual mechanism of cAMP-induced desensitization of the AC pathway. While more elaborate models can perform better when simulating certain experimental procedures, the two-variable model incorporated here certainly captures the essence of the cAMP signalling system in *Dictyostelium*: fast cAMP production in a positive feedback loop and slow cAMP-induced desensitization. In a spatially extended (2D) medium with cAMP diffusion as the only transport process, the system has the typical properties of an excitable medium, and in particular supports stable spiral wave solutions (Figure 1) [14,18]. In addition, a slight shift in parameters (for example an increase in AC activity [13]) can cause amoebae to produce cAMP in a periodic fashion. This is what normally happens at the beginning of aggregation when the establishment of a number of autonomously oscillating centres (pacemakers) can be observed. From these the cAMP signal is relayed as a series of expanding concentric waves. Inhomogeneities in the medium can break these waves, and the resulting free wave tips give rise to cAMP spirals.

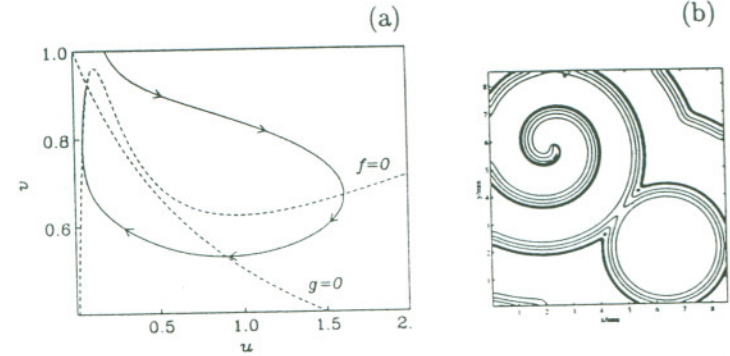


Figure 1: Behaviour of system (2)–(3) with cell density “clamped” at a constant value ( $n = 1.0$ ); (a) phase plane with typical excitation trajectory, and (b) contour plot of spiral wave solution (upper left of domain) and concentric wave (lower right; the pacemaker region in the centre is silent at the time of the snapshot) on a two-dimensional spatial domain. Nondimensional parameters:  $\lambda = 70.0$ ,  $a = 0.0014$ ,  $b = 0.2$ ,  $d = 0.0234$ ,  $\delta = 0.11$ ,  $k_{+} = k_{-} = 2.5$ ,  $D = 1.0$ ; timescale 2.5 min, length scale 220  $\mu\text{m}$ , cAMP scale  $5 \times 10^{-7}$  M.

However, in previous models these wave solutions have been obtained with the idealization of a stationary homogeneous cell layer. We now turn to the investigation of the full model (1)–(3) which includes the dynamics of the cell distribution.

#### 4 Cell streaming—the patterning mechanism

As discussed above, equations (2)–(3), with cell density viewed as a constant and spatially homogeneous parameter, exhibit travelling wave solutions and, in particular, spiral waves. For the full model (1)–(3) it can be shown that travelling wave solutions again exist, which are almost identical to the wave solutions obtained for cell density “clamped” at a constant value. The reason for this is essentially the very small ratio of typical cAMP wavespeed (300  $\mu\text{m}/\text{min}$ ) to chemotactic (advective) cell velocity (20  $\mu\text{m}/\text{min}$ ). From equation (1) an estimate for the disturbance of a homogeneous cell distribution,  $n_0 = \text{constant}$ , in the front of a cAMP wave can be obtained as  $n \approx n_0/(1 - w/c)$ , where  $c$  and  $w$  denote the cAMP wavespeed and the average chemotactic cell velocity, respectively. Thus wave-induced cell movement leaves the homogeneous cell layer practically undisturbed—an observation also reported for the *in situ* situation [19].

Therefore the basic ideas on the initiation of pattern formation by cAMP waves carry over to the full model incorporating cell movement. However, we

shall show that there is a crucial difference between the density-clamped case and the full model: Whereas the cAMP spiral waves and periodically forced target patterns constitute stable dynamical attractors in the previous models, they will function as a slowly evolving “chemical prepattern” for cellular morphogenesis when cell chemotaxis is included.

This can be best understood by considering the stability of the wave solutions in the full model. For this purpose one looks at the evolution of a small perturbation of the wave solution with time. Such perturbations are naturally supplied by small random inhomogeneities in the cell distribution. The linear stability analysis of the model around two-dimensional periodic wave solutions is carried out in detail in [20]. It essentially reduces to considering a linear problem of the form

$$\frac{da(z; q^2)}{dz} = A(z; q^2) a(z; q^2); \quad z = x + ct. \quad (4)$$

Here periodic plane waves are assumed to propagate in  $x$ -direction with speed  $c$ , hence  $z$  denotes a coordinate frame moving with the waves:  $a(\cdot; q^2)$  denotes the amplitude of the  $q$ -th Fourier mode of a spatial perturbation of the system variables in the  $y$ -direction, that is *perpendicular* to the direction of wave propagation. Hence the total perturbation in the  $y$ -direction is

$$\text{perturbation}(y, z) = \int a(z; q^2) \exp\{iqy\} dq \quad (5)$$

Whether a perturbation with a certain spatial wavelength  $2\pi/q$  will grow or decay with time depends on the evolution of its amplitude which is determined by (6). The system matrix  $A(z; q^2)$ , the actual form of which is derived in [20], is periodic in  $z$  through a dependence on the unperturbed periodic wave solutions of (1)–(3), that is, the evolution of the perturbation is *forced by the periodic cAMP waves*. This is further emphasized by the fact that the time-like variable in (6) and (7) is the travelling wave variable  $z$ : the perturbation essentially evolves in the travelling wave frame. Standard Floquet theory can be employed to obtain the *dispersion relation* from (6), that is the graph of the characteristic linear growth rates of the Fourier modes [20]. The result is depicted in Figure 2. One can clearly see that there is a band of unstable spatial wavenumbers. Thus cAMP wave propagation in the initially homogeneous cell layer is unstable from the outset, and the waves force the slow growth of a pattern parallel to the wavefronts with a characteristic length scale roughly an order of magnitude larger than the typical cell diameter. As we shall see in the next section, it is this patterning instability which gives rise to cell streams observed *in situ*. A more detailed investigation of the instability mechanism

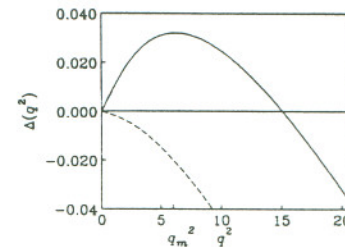


Figure 2: Dispersion relation for patterning parallel to cAMP wavefronts resulting from (6). The ordinata measures the linear growth rate of the spatial Fourier modes given on the abscissa. The solid line is obtained with the parameters given in Figures 3 and 5; there is a band of unstable wavenumbers (small positive growth rates). The dashed line corresponds to a weaker chemotactic response  $\chi_0 = 0.2$ ; here the uniform cell layer is stable.

uncovers the typical features of a *chemotaxis-driven instability* [12], in the present case forced by periodic chemoattractant waves [20]. We conjecture from the linear analysis that cAMP wave propagation gives rise to a slow break-up of the initially homogeneous cell layer perpendicular to the direction of wave propagation, that will eventually lead to the formation of a cell stream pattern.

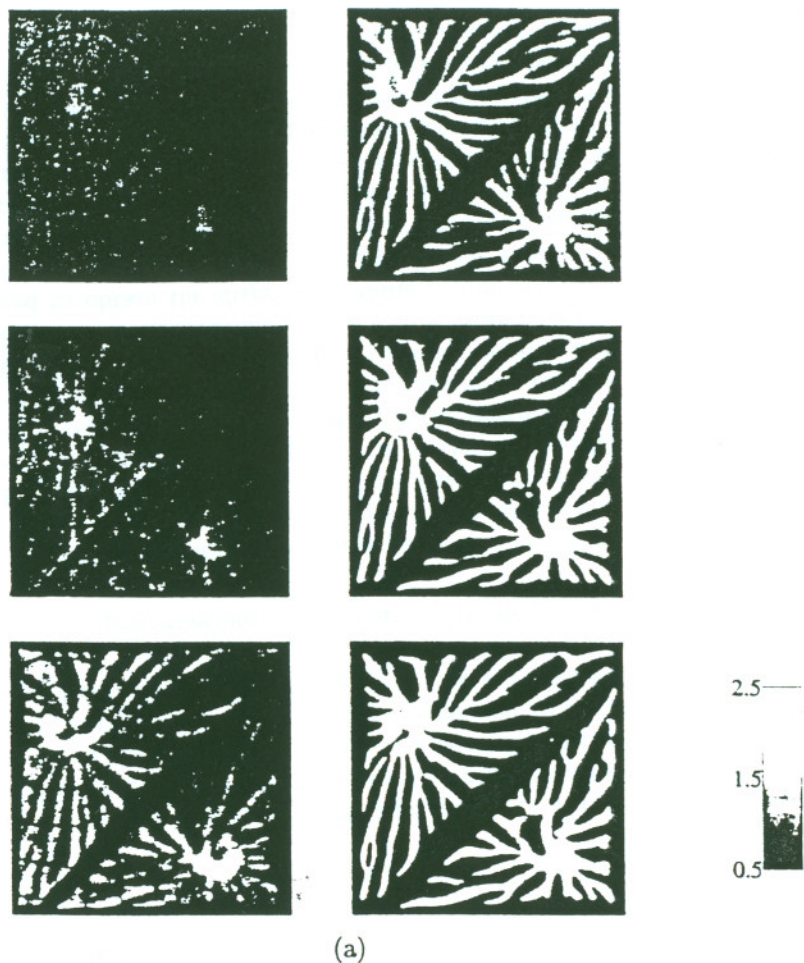
## 5 Numerical explorations

To investigate the instability mechanism in the fully nonlinear model, we solve (1)–(3) numerically. A standard finite difference discretization on a rectangular domain is employed, with an alternating direction implicit scheme for the diffusion operator and an upwind scheme for the chemotaxis term.

A typical simulation result is shown in Figure 3. One clearly sees the development of a counter-rotating spiral pair from a disrupted wavefront, the partitioning of the domain in two distinct aggregation territories roughly along the diagonal, and finally the break-up of the cell layer into a pattern of branching cell streams, that is, the onset of multicellularity. During cell stream development the cAMP waves retain their principal spiral geometry, though with an increasingly rugged and irregular concentration profile (Figure 3 (b)).

Thus the model (1)–(3) captures the essential dynamics of aggregation, and we can now proceed to compare different model predictions with the results of the linear analysis and experimental observations.

(i) *Cell streams arise on a characteristic spatial scale*



(a)

Figure 3: Spatio-temporal evolution of (a) cell density, and (b) cAMP concentration in a numerical simulation of system (1)–(3). The dimensional domain size is as in Figure 3 (b); snapshots are taken in intervals of 15 min (from top left downwards, to bottom right). Initially a small random perturbation between  $-0.075$  and  $0.075$  was added to the homogeneous cell density ( $1.0$ ) at every mesh point. Boundary conditions are zero-flux. Parameters as in Figure 3, and  $\mu = 0.012$ ,  $\chi_0 = 0.5$ ,  $A = 0.72$ ,  $m = 10.0$ ,  $\rho = 0.7$  and  $K = 0.8$ ; reference cell density  $1.5 \times 10^{-4}/\text{cm}^2$



(b)

Figure 3: continued.

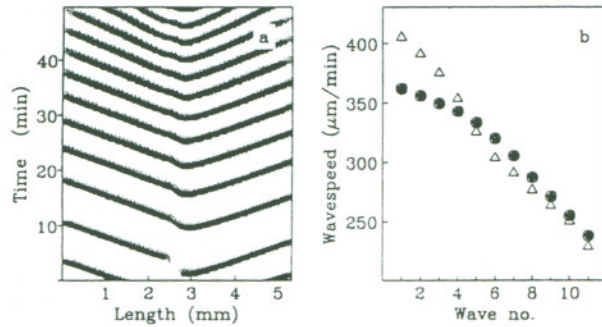


Figure 4: (a) Evolution of cAMP concentration in a spatial slice through an aggregation territory with a cAMP spiral; (b) corresponding wave velocities (●), compared to the experimental data in [21], Figure 3 (Δ). The spatial slice is taken parallel to the horizontal boundary through the spiral wave core.

The power spectrum of the evolving small-amplitude pattern in cell distribution clearly shows a distribution of modes around a dominant spatial frequency ([20], Figure 7). This agrees with the analytical prediction of a dispersion relation with a single maximum. Moreover, the numerical values for the dominant modes are in good agreement [20]. Obviously, such a characteristic spatial scale together with the spiral or concentric geometry of the cAMP waves provides a recipe for the formation of a branching stream pattern. Quantitative *in situ* data do not exist, but within an aggregation territory streams usually appear to be distributed around a characteristic width. Both a certain “freezing” of initial inhomogeneities and nonlinear competition are familiar phenomena in chemotaxis systems which can contribute to such a width distribution, which is also seen in the simulations.

(ii) *Spiral period and wavespeed depend on “wave time”*

It has long been recognized that the basic geometry of the cAMP spiral waves changes as aggregation proceeds: the wave frequency increases while the propagation speed drops [21]. This behaviour, which has not been observed in any other excitable medium, has been attributed to somewhat speculative biochemical changes which are thought to be stimulated directly by the cAMP waves. However, our minimal model exhibits this phenomenon with constant parameter values (Figure 4). This certainly does not rule out slow biochemical modifications which may enhance it [5]. On the other hand, the model (1)–(3) offers an explanation of the basic phenomenon within the framework of

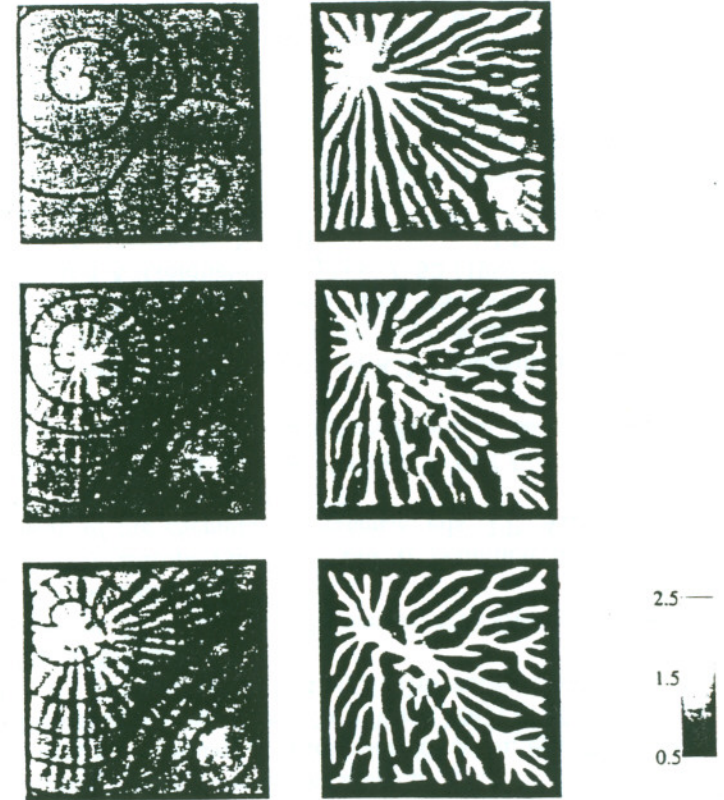


Figure 5: Competition of two aggregation territories, organized by a spiral wave of cAMP and a periodic pacemaker. Shown is the cell density, and in the first three snapshots also the cAMP wave contours. Details of simulation as in Figure 3.

excitable media in terms of slowly evolving inhomogeneous excitability properties of the cell layer, caused by aggregation and streaming [10,20].

(iii) *Caffeine induces rotating cell loops*

Caffeine is known as a pharmacological agent to affect both aggregation and subsequent development. It inhibits the AC pathway [22], and applied in large quantities stops cAMP wave propagation (P. Newell, personal communication). A simulation of moderate caffeine application, reflected in a decrease of the activity of the AC pathway by about 25 %, shows the formation of a cell loop in the centre of the aggregation territory; cf. [10], Figure 5. The core of the cAMP spiral continuously cycles around this cell loop and consequently

22. M. Brenner and S. Thoms, *Devl. Biol.* **101** (1986) 136.
23. A.S. Mikhailov, *Foundations of Synergetics* (2nd ed.), (Springer-Verlag, Berlin, 1994).
24. M.C. Boerlijst and P. Hogeweg, *Physica D* **48** (1991) 17.
25. A.M. Turing, *Phil. Trans. Roy. Soc. Lond. B* **237** (1952) 37.
26. J.D. Murray, *Mathematical Biology* (Springer, Berlin, 1989).
27. G.C. Cruywagen, P.K. Maini, J.D. Murray, *IMA J. Math. Appl. Med. Biol.* **9** (1992) 227.
28. R.J. Keynes and C.D. Stern, *Development* **103** (1988) 413.
29. F. Siegert, C.J. Weijer, A. Nomura, H. Miike, *J. Cell Sci.* **107** (1994) 97.

## CONCERTED REGULATION OF CYCLIC ADENOSINE MONOPHOSPHATE BY CALMODULIN/CALCIUM COMPLEX AND DOPAMINE: A KINETIC MODELLING APPROACH

ROLF KÖTTER, DIRK SCHIROK, and KARL ZILLES  
C. & O. Vogt Institute for Brain Research, Heinrich Heine University,  
PO Box 101007, D-40001 Düsseldorf, Germany

### Introduction

The complex role of biochemical pathways in the intracellular mediation of synaptically induced effects in neurons is increasingly being recognized. The analysis of such pathways has much to offer, particularly in respect to the non-classical transmitters that exert "modulatory" metabotropic effects in the central nervous system. Such a "modulatory" transmitter is dopamine, which is known to influence intracellular cyclic adenosine monophosphate (cAMP) concentrations in the striatum via G proteins and adenylate cyclase (AC)<sup>1</sup>. However, cAMP levels are also affected by calcium<sup>2,3</sup>, a second messenger whose intracellular concentration increases, for example, in response to synaptically released glutamate<sup>4,5</sup>. A previous equilibrium model of dopamine and calcium interactions in the mammalian striatum provided important insights into distinct concentration-dependent modes of postsynaptic signal integration<sup>6</sup>. Here we present a kinetic model of cAMP regulation by calmodulin/calcium complex and dopamine via AC and phosphodiesterase (PDE) in order to further investigate the responses of intraneuronal cAMP concentrations to brief calcium and dopamine pulses.

### Methods

An established scheme of intracellular second messenger pathways was adopted in the present study<sup>6-8</sup> (Fig. 1): As a first approximation, AC activity in the striatum is controlled by three factors: It is stimulated by dopamine (DA) and calmodulin/calcium complex (CaM<sub>Ca</sub>4), and inhibited by intracellular free calcium (Ca). Adenylate cyclase forms cAMP from its substrate adenosine triphosphate (ATP). Cyclic AMP is hydrolyzed to AMP by phosphodiesterase (PDE), whose activity depends on CaM<sub>Ca</sub>4.

22. M. Brenner and S. Thoms, *Devl. Biol.* **101** (1986) 136.
23. A.S. Mikhailov, *Foundations of Synergetics* (2nd ed.), (Springer-Verlag, Berlin, 1994).
24. M.C. Boerlijst and P. Hogeweg, *Physica D* **48** (1991) 17.
25. A.M. Turing, *Phil. Trans. Roy. Soc. Lond. B* **237** (1952) 37.
26. J.D. Murray, *Mathematical Biology* (Springer, Berlin, 1989).
27. G.C. Cruywagen, P.K. Maini, J.D. Murray, *IMA J. Math. Appl. Med. Biol.* **9** (1992) 227.
28. R.J. Keynes and C.D. Stern, *Development* **103** (1988) 413.
29. F. Siegert, C.J. Weijer, A. Nomura, H. Miike, *J. Cell Sci.* **107** (1994) 97.